

Model reconstructions for the Si(337) orientation

F C . Chuang^a, C V . C ioianu^b, C Z . W ang^a, and K M . H o^a

^aAmes Laboratory { U S . D epartment of E nergy and

D epartment of Physics, Iowa State University, Ames, Iowa 50011, USA

^bD ivision of E ngineering, Colorado School of M ines, Golden, Colorado 80401, USA

November 1, 2019

Abstract

Although unstable, the Si(337) orientation has been known to appear in diverse experimental situations such as the nanoscale faceting of Si(112), or in the case of miscutting a Si(113) surface. Various models for Si(337) have been proposed over time, which motivates a comprehensive study of the structure of this orientation. Such a study is undertaken in this article, where we report the results of a genetic algorithm optimization of the Si(337)-(2 1) surface. The algorithm is coupled with a highly optimized empirical potential for silicon, which is used as an efficient way to build a set of possible Si(337) models; these structures are subsequently relaxed at the level of ab initio density functional methods. Using this procedure, we retrieve most of the (337) reconstructions proposed in previous works, as well as a number of novel ones.

Corresponding author. Email: cciobanu@mines.edu, Phone: 303-384-2119, Fax: 303-273-3602

1 Introduction

Silicon surfaces have been at the foundation of the semiconductor industry for several decades. With the advent of nanotechnology, the interest in the atomic structure of various semiconductor surfaces has expanded because of their potential to serve as natural and inexpensive templates for growing various types of nanostructures. Understanding the growth of nanoscale entities on various substrates depends, at least in part, on knowing the atomic structure of the substrate; given that low-index crystal surfaces are well understood, the high-index surfaces are now progressively gaining importance as their richer morphological features may lead to novel applications. To date, there are numerous stable high-index orientations reported in the literature; in the case of Silicon and Germanium, these stable orientations have been summarized in Ref. [1]. The unstable high-index orientations are important in their own right, as they often give rise to remarkable periodic grooved morphologies which may be used for the growth of surface nanowires. The wonderful morphological and structural diversity of high-index surfaces can be appreciated, for instance, from the work of Baski, Ew in and W himan, who investigated systematically the surface orientations between Si(001) and Si(111) [2].

An interesting case of unstable surface is Si(337), whose atomic structure is the subject of the present article. As a historical account, we note that the Si(337) orientation was concluded to be stable in early studies by Ranke and Xing [3], Gardieniers et al. [4], and Hu et al. [5]. This conclusion about the stability of Si(337) was consistent with the reports of Baski and W himan, who showed that Si(112) decomposes into quasi-periodic Si(337) and Si(111) nanofacets [6], and that Si(337) is a low-energy orientation [7]. However, further studies by Baski and W himan revealed that Si(337) itself facets into Si(5 5 12) and Si(111) [8], demonstrating that Si(337) was, in fact, unstable. Since Si(337) is not stable and Si(5 5 12) is [9, 10], the clean Si(112) orientation should facet into Si(5 5 12) and Si(111); yet, as explained in Ref. [8], nanofacets are too narrow to form complete Si(5 5 12) units, and mostly settle for the nearby Si(337) orientation. A more recent report [11] shows another situation where Si(337) arises rather than the expected Si(5 5 12). For a Si(113) surface that is miscut towards [111], the large (5 5 12) reconstruction has not always been found; instead, a Si(337) phase has been seen to coexist with Si(113) terraces [11]. The high resolution transmission electron microscope (HRTEM) images in [11] leave no doubt that the periodicity of those nanofacets corresponds to the (337) orientation. The reason for the quasi-stability of Si(337) reported in earlier works [3, 4, 5] could be the curvature or the size of substrates used in those investigations; this explanation is also consistent with Ref. [11], where the issue of sample curvature is acknowledged.

With one exception [5], atomic-scale models for Si(337) were not sought separately, but rather as structural parts of the Si(5 5 12)-(2 1) reconstruction [9, 12, 13, 14]. As shown in Ref. [9], the Si(5 5 12) unit cell consists of two Si(337) units and one Si(225) unit. The first model reconstruction proposed for Si(5 5 12) [9] appeared somewhat corrugated when viewed along the [110] direction; so did a second model by Ranke and Xing [12]. On the other hand, HRTEM measurements [13] showed a better profile for Si(5 5 12), and new model

reconstructions were proposed [13, 14] in order to account for the observed flatness. Total-energy density functional calculations for Si(5 5 12) have only recently been reported, and suggest that the latest models [13, 14] have lower energies than the earlier proposals [9, 12].

The reason structural studies of high-index surfaces can be very lengthy originates from the way model reconstructions are proposed, which is based on physical intuition in interpreting scanning tunneling microscope (STM) images. As seen above for the case of Si(5 5 12), the intuitive ways are not very robust for high-index surfaces, since usually more models are required when new experimental data becomes available. Given the rather large number of low-energy structures that high-index surfaces can have (see, e.g., the case of Si(105) [15, 16]), heuristic approaches pose the risk of missing the actual physical reconstruction when considering model candidates for comparison with the experimental data. To alleviate this risk, we have recently addressed the reconstruction of semiconductor surfaces as a problem of stochastic optimization [16], and developed two different global search algorithms for the purpose of determining the most favorable surface structure [16, 17]. We have used these global search procedures for studying Si(105) [16, 17] and Si(114) [18], which are both stable orientations for silicon. Si(337) is not stable [8], but its atomic structure can still be pursued with global search algorithms because the only input required is the periodic vectors of the surface; these vectors are available from STM [9] and LEED [5] measurements. In this article we report the results of such a global optimization for the structure and energy of Si(337) using empirical potential and density functional theory calculations. As we shall see, the optimization retrieves most of the models proposed previously [5, 9, 13, 14], as well as a number of other reconstructions that could be relevant for experimental situations where Si(337) nanofacet arises (other than the two (337) unit cells that appear as part of the (5 5 12) structure).

The remainder of this article is organized as follows. In the next section we briefly describe the computational methods used in this study. In Section 3, we present our model structures for the Si(337) surface classified by the number of atoms in the computational cell and their surface energy. We compare our results with Si(337) other reported models in Section 4. Our conclusions are summarized in last section.

2 Methods and Computational details

The Si(337) simulation cell consists of two (337) bulk truncated unit cells of dimensions $a = 8.375$ $a = 0.5$ $a = 6.7$, (a is the lattice constant of Si), stacked along the y -direction, $\bar{[110]}$. These dimensions are calculated from the crystal geometry, and are in agreement with the STM images published in Ref. [9], where (337) units are shown as part of a stable reconstructed surface, Si(5 5 12)-(2 1). Because the (337) plane has two-dimensional periodicity along two non-orthogonal directions, the rectangular unit in Fig. 1 must be subjected to shifted periodic boundary conditions [19], with the shift in the y -direction equal to $a = \frac{p}{8}$.

We build a database of structures sorted out by the number of atoms in the simulation

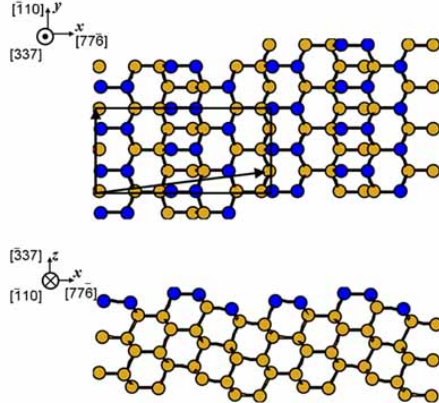


Figure 1: (Color online) Top and side view of the unreconstructed Si(337) surface. The rectangle represents the simulation cell that is subjected to shifted periodic boundary conditions [19], and the solid arrows are the corresponding periodic vectors; four such periodic cells are shown in the figure in order to aid the eye with the shifted boundary conditions. The darker shade marks the undercoordinated surface atoms.

cell and by their surface energy calculated with the highly optimized empirical potential developed by Lenosky et al. [20]. The number of atoms is varied around the initial value of $n = 268$, to exhaust the number of distinct possibilities that can occur during the search for low energy reconstructions.

The global optimization involved in building the structure database for Si(337) has been performed with the genetic algorithm adapted for crystal surfaces [17]. This algorithm is based on an evolutionary approach in which the members of a generation (pool of models for the surface) evolve with the goal of producing the best specimens, i.e. lowest energy reconstructions. The evolution from one generation to the next takes place by mating, which is achieved by subjecting two randomly picked structures (parents) from the pool to an operation that combines their surface features and creates a child con guration. This child structure is relaxed and considered for inclusion in the pool, depending on its surface energy. We use two variants of the algorithm, one in which the number of atoms is kept constant for all members of the pool at all times (the constant- n version), and another one in which this restriction is not enforced (the variable- n version). The implementation of this genetic algorithm has recently been described in various degrees of detail in Refs. [17, 18, 21]; for this reason, we will not expand upon it here, but refer the reader to those works. Since the empirical potentials may not give a very reliable energy ordering for a database of structures, we study not only the global minimum in a given by HOEP for different values of n , but also most of the local minima that are within 15 meV/ \AA^2 from the lowest energy configurations. After

creating the set of Si(337) model structures via the genetic algorithm, we recalculate the surface energies of these minima at the level of density functional theory (DFT).

The DFT calculations were performed with the plane-wave based PW scf package [22], using the Perdew-Zunger [23] exchange-correlation energy. The cutoff for the plane-wave energy was set to 12 Ry, and the irreducible Brillouin zone was sampled using 4 k-points. The equilibrium bulk lattice constant was determined to be $a = 5.41\text{ \AA}$, which was used for all the surface calculations in this work. The simulation cell has the single-face slab geometry with a total silicon thickness of 10 \AA , and a vacuum thickness of 12 \AA . The Si atoms within a 3 \AA -thick region at the bottom of the slab are kept fixed in order to simulate the underlying bulk geometry, and the lowest layer is passivated with hydrogen. The remaining Si atoms are allowed to relax until the force components on any atom become smaller than $0.025\text{ eV}/\text{\AA}$.

The surface energy for each reconstruction is determined indirectly, by first considering the surface energy σ_0 of an unrelaxed bulk truncated slab, then by calculating the difference

$\Delta\sigma = \sigma - \sigma_0$ between the surface energy of the actual reconstruction and the surface energy of a bulk truncated slab that has the bottom three layers fixed and hydrogenated. This indirect method for calculating the surface energies at the DFT level was outlined, for instance, in Ref. [25]. The energy of the bulk truncated surface shown in Fig. 1 was found to be $\sigma_0 = 137.87\text{ meV}/\text{\AA}^2$. At the end of the genetic algorithm search, we obtain a set of model structures which we sort by the number of atoms in the simulation cell and by their surface energy. These model structures are presented next.

3 Results

There are four possibilities in terms of the number of atoms in the slab that yield distinct global energy minima of the Si(337) periodic cell shown in Fig. 1. This has been determined by performing constant- n genetic optimization for computational slabs with consecutive numbers of atoms n ($264 \leq n \leq 272$), and identifying a periodic behavior of the surface energy as a function of n ; this way of determining the symmetry distinct numbers of atoms in the computational slab has been detailed in Ref. [16]. The HOEP global minima, as well as selected local minima of the surface energy for different numbers of atoms are summarized in Table 1, along with the density of dangling bonds per unit area and the surface energy computed at the DFT level.

As a general comment, the DFT energy ordering does not coincide with that given by HOEP, indicating that the transferability of HOEP to Si(337) is not as good as in the case of Si(001) and Si(105); to cope with this transferability issue, we have considered more local minima (than listed in Table 1) when performing DFT relaxations, as mentioned in Section 2. In the terminology of potential energy surface (PES) theory, we sample the main basins using the genetic algorithm coupled with HOEP, then recalculate the energetic ordering of these basins using DFT. From the table it is apparent that the least favorable number of atoms is $n = 267$ (modulo 4) at both the HOEP and DFT levels. Therefore, we focus on describing

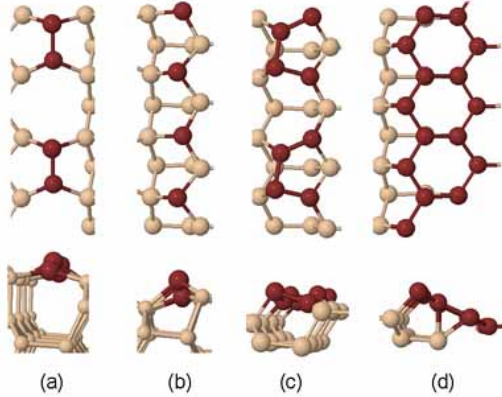


Figure 2: (Color online) Structural features (top and side views) that can be present on low-energy Si(337) reconstructions: (a) dimers, (b) rebonded atoms, (c) tetramers, and (d) honeycombs. In each case, the atoms that make up the feature are darker.

here the reconstructions that have numbers of atoms $n = 266, 268$, and 269 .

For $n = 266$ the best model that we obtained at the DFT level is made of a fused assembly of dimers, tetramers and slightly puckered honeycombs, followed (in the $[7\bar{7}\bar{6}]$ directions) by a row of rebonded atoms; these individual atomic-scale features have been reported previously for different surfaces (e.g., [9, 14, 24]), and depicted for convenience in Fig. 2. Their complex assembly is shown in Fig. 3(a), and has a surface energy of $94.47 \text{ m eV}/\text{Å}^2$; this novel reconstruction has a corrugated aspect when viewed from the $[\bar{1}10]$ direction, which makes it relatively unfavorable. Three higher-energy models with $n = 266$ are illustrated in Fig. 3(b,c,d), and have surface energies ranging from $2.75 \text{ m eV}/\text{Å}^2$ to $6.96 \text{ m eV}/\text{Å}^2$ above the surface energy of the model in Fig. 3(a). The structural features of these local minima are clearly identifiable as tetramers and dimers [Fig. 3(b)], and rebonded atoms and honeycombs [Fig. 3(c)].

The optimum number of atoms is $n = 268$, as indicated in Table 1 at both HOEP and DFT levels (coincidentally, this is also the number of atoms that corresponds to two complete (337) bulk truncated primitive cells. We have further verified this number by performing a variable- n genetic algorithm started with all the members in the pool initially having $n = 267$ atoms. The algorithm retrieved the correct number of atoms ($n = 268$) and the HOEP global minimum in less than 1000 operations; while different starting configurations may change this rather fast evolution towards the global minimum, our tests indicate that for simulation cells of similar size several thousand genetic operations are sufficient when using the implementation in Ref. [17]. The lowest energy model as given by DFT is shown in Fig. 4(a) and consists of dimers, rebonded atoms and honeycombs, in this order along $[7\bar{7}\bar{6}]$. We note that the number of dangling bonds is smaller at the DFT level: the reason for the dangling bond reduction is the

n	Bond counting (db/ a^2) <u>16:75</u>	H O E P (m eV / \AA^2)	D F T (m eV / \AA^2)	Fig.
266	10 (10)	87.37	109.04	
	10 (10)	87.74	97.22	3 (b)
	6 (4)	87.79	100.39	3 (c)
	10 (10)	89.60	102.35	
	4 (3)	92.07	94.47	3 (a)
	4 (4)	93.87	101.43	3 (d)
267	8 (8)	92.35	99.95	
	8 (8)	92.37	96.47	
	10 (8)	92.47	107.72	
	9 (8)	99.11	101.33	
268	8 (6)	81.99	93.13	4 (c)
	8 (8)	83.11	95.17	
	8 (6)	83.43	89.61	4 (b)
	8 (8)	84.90	94.52	4 (d)
	8 (6)	85.47	90.19	
	8 (6)	85.94	89.12	4 (a)
269	4 (4)	89.18	93.50	5 (a)
	6 (6)	92.58	99.21	5 (b)

Table 1: Surface energies of different Si(337)-2 1 reconstructions, sorted by the number of atoms n in the periodic cell. The second column shows the number of dangling bonds per unit area, counted for structures relaxed with HOEP; the dangling bond density at the DFT level is shown in parentheses. Columns three and four list the surface energies given by the HOEP potential [20] and by density functional calculations (DFT) [22] with the parameters described in text.

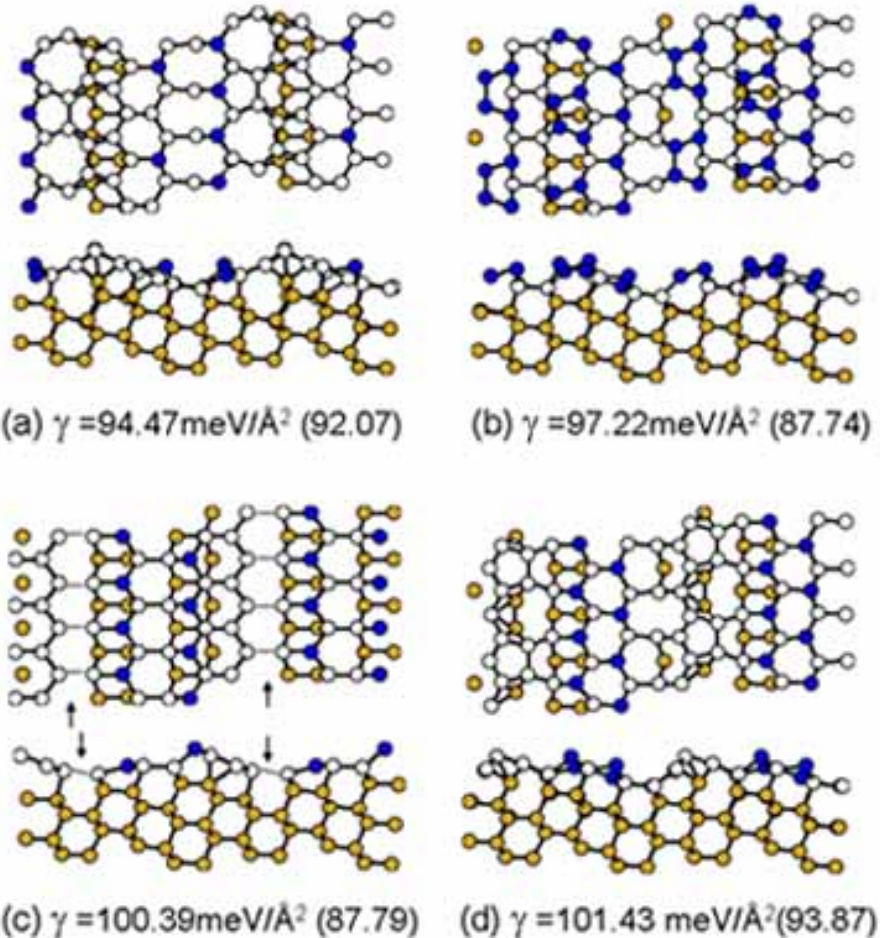


Figure 3: (Color online) Models of Si(337) reconstructions with $n = 266$ atoms per (2×1) unit cell, after DFT relaxation (top and side views). The surface energy computed from first-principles is indicated for each structure, along with the corresponding value (in parentheses) determined with the HOEP interaction model [20]. The dark blue marks the undercoordinated atoms. The four-coordinated atoms that are exposed at the surface are shown in white.

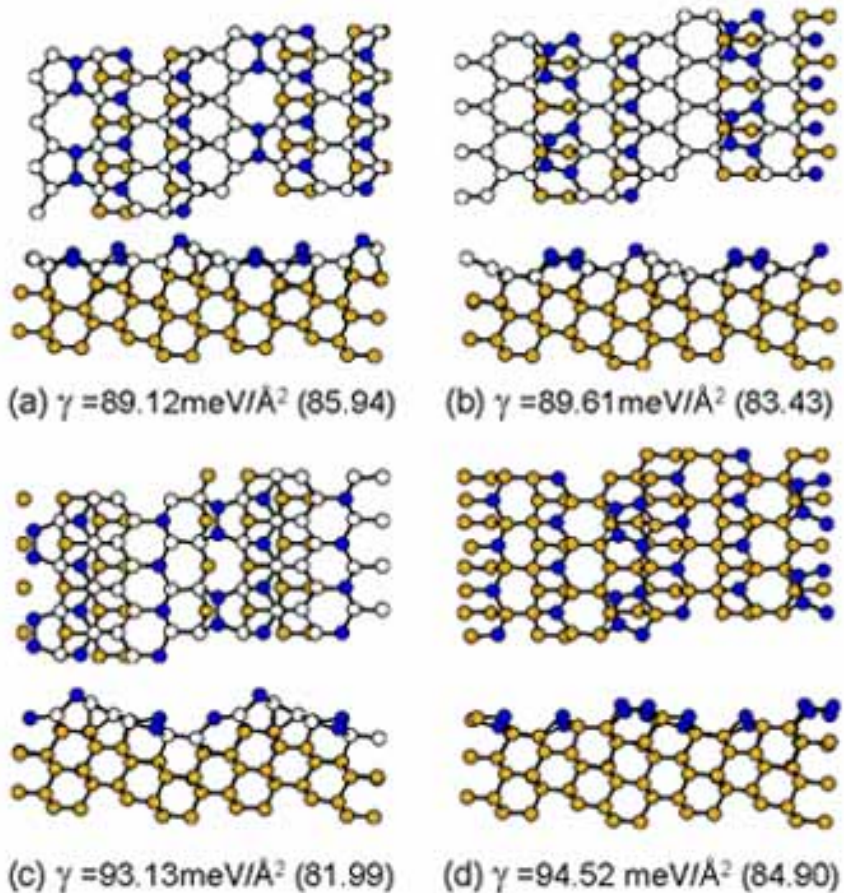


Figure 4: (Color online) Models of Si(337) reconstructions with $n = 268$ atoms per (2×1) unit cell, after DFT relaxation (top and side views). The surface energy computed from first-principles is indicated for each structure, along with the corresponding value (in parentheses) determined with the HOEP interaction model [20]. The dark blue marks the undercoordinated atoms, while the four-coordinated atoms that are exposed at the surface are shown in white. The lowest-energy Si(337)-(2 \times 1) reconstructions are shown in (a) and (b); these structures differ in the position of the dimer row in the unit cell, which can form a -bonded chain followed by a row of rebonded atoms (a), or it can combine with those rebonded atoms to form a tetramer row (b).

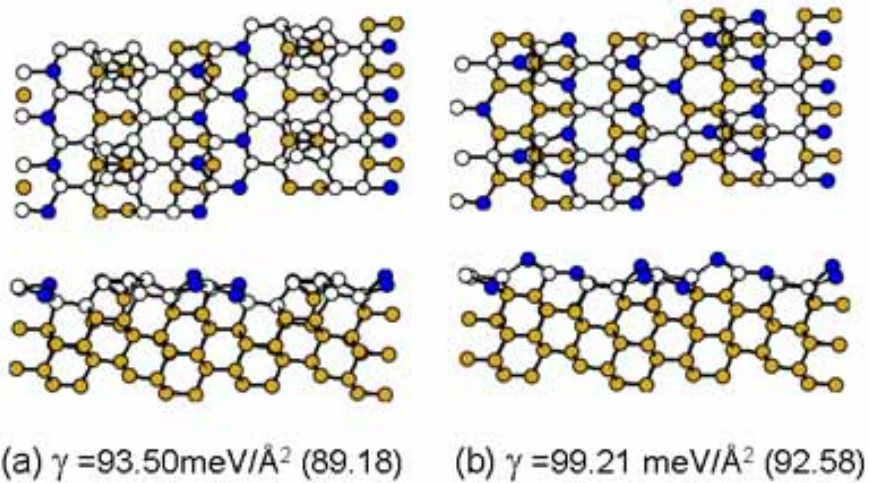


Figure 5: (Color online) Models of Si(337) reconstructions with $n = 269$ atoms per (2×1) unit cell, after DFT relaxation (top and side views). The surface energy computed from first-principles is indicated for each structure, along with the corresponding value (in parentheses) determined with the HOP model [20]. The dark blue marks the undercoordinated atoms, while the four-coordinated atoms that are exposed at the surface are shown in white. In (a), we note the presence of pentamers stabilized by subsurface interstitials.

attening of the honeycombs (not planar at the level of empirical potentials), which creates two additional bonds with the subsurface atoms. The genetic algorithm search retrieves another low-energy model, in which the dimers are displaced towards and combine with the rebonded atoms forming tetramers [Fig. 4(b)]. The two models in Figs. 4(a) and (b) are nearly degenerate, with a surface energy difference of 0.5 m eV / \AA^2 relative to one another. A different ordering of the features in Fig. 4(a) gives rise to a noticeably larger surface energy: specifically, the arrangement of dimers, honeycombs and rebonded atoms [Fig. 4(c)] increases the surface energy by 4 m eV / \AA^2 relative to the model in 4(a). An even higher-energy model made up of tetramers and rebonded atoms is shown in Fig. 4(d).

When the number of atoms in the simulation cell is $n = 269$, we find that the ground state is characterized by the presence of surface pentamers and rebonded atoms [refer to Fig. 5(a)]. Interestingly, this structure is nearly flat, with the rebonded atoms being only slightly out of the plane of the pentamers; these pentamers are "supported" by six-coordinated subsurface interstitials. For the Si(337) cell with $n = 269$ atoms, we find a very strong stabilizing effect of the pentamer-interstitial configuration: the next higher-energy structure [Fig. 5(b)] is characterized by ad-atoms and rebonded atoms, with a surface energy that is 5 m eV / \AA^2 higher than that of the ground state in Fig. 5(a). We note that subsurface interstitials have long been reported to have a stabilizing effect for the reconstructions of Si(113), (3 1) and (3 2) [25]. Next, we compare the structural models described above with previously published works on the Si(337) structure.

4 Discussion

The first model of Si(337) reconstruction [5, 9] was based on pairing the atoms of the bulk truncated structure [Fig. 1] by displacing them along $\bar{[1}10]$ such as to form dimers and tetramers. This model is retrieved by the genetic search with $n = 266$ [Fig. 3(b)], and has a high density of dangling bonds (db) per unit area, 10 db / \AA^2 [16:75]. While the high dangling bond density may seem to suggest a high surface energy, a close inspection of Table 1 shows that, in fact, there is no clear correlation between the dangling bonds and the surface energy. If we take the DFT model 3(a) as reference, we note that an increase of one db per unit cell [from 3(a) to 3(c)] results in a surface energy increase of 7 m eV / \AA^2 ; on other hand, an increase of seven db in the simulation cell [from 3(a) to 3(b)] increases the surface energy by less than 3 m eV / \AA^2 . Similar arguments for the lack of correlation between missing bonds and surface energy can be made by analyzing structures with other numbers of particles in Table 1. For example, at the optimum number of atoms ($n = 268$), we find that with the same dangling bond density, models 4(a)-(c) span a 4 m eV / \AA^2 surface energy range: this range is so large that it includes the global minimum as well as higher surface energy local minima that may not be observable in usual experiments. These findings are consistent with the fact that the minimization of surface energy is not controlled solely by the reduction of the dangling bond density, but also by the amount of surface stress caused in the process [9]. Given that the heuristic approaches

may only account for the dangling bond density when proposing candidate reconstructions, the need for robust minimization procedures (e.g., [16, 17]) becomes apparent.

The configuration with the lowest number of dangling bonds ($3db/a^2 = 16.75$) is shown in Fig. 3(c), where the bonds that join the (lower corner of) honeycombs and the neighbors of the rebonded atoms are markedly stretched beyond their bulk value: the stretched bonds [indicated by arrows in Fig. 3(c)] cause the surface energy to become very high, $100.39 \text{ m eV}/\text{A}^2$ at the DFT level. Interestingly, the surface stress is very efficiently relieved by adding dimers such that stretched bonds are broken, and the dimers "bridge" over as shown in Fig. 4(a). The addition of one dimer per simulation cell results in the most stable Si(337) reconstruction that we found, with $89 \text{ m eV}/\text{A}^2$. A model similar in topology with 4(a) was proposed by Liu et al. [13] to explain their HRTEM data; these authors also proposed a possible configuration for the other unit of (337) that is part of the large Si(5 5 12) reconstruction, which has essentially the same bonding topology as 4(b). Although no atomic scale calculations were performed in [13], the two (337) models of Liu et al. were in qualitative agreement with more recent DFT results by Jeong and coworkers [14], as well as with STM and HRTEM images; when performing ab-initio relaxations, we found that the initial HOEP model structures that corresponded most closely to those in Ref. [13] end up relaxing into the configurations put forth by Jeong and coworkers [14]. The configurations shown in Fig. 4(a,b) allow for (337) nanofacets to intersect (113) facets without any bond breaking or rebonding [11]. This absence of facet-edge rebonding, as well as the relatively low energy of Si(337), give rise to short-range attractive interactions between steps on miscut Si(113) [26], which is consistent with the experimental observation of (337) step-bunched phases [11].

5 Conclusions

In summary, we have presented an investigation of the Si(337)-(2 1) reconstructions based on a genetic algorithm [17, 21] search for the most favorable atomic configuration. We have coupled the algorithm with the HOEP model [20] for atomic interactions in order to efficiently create a database of Si(337) models. Since no empirical interatomic potential can be expected to be fully transferable to arbitrary surface orientations, we have relaxed the database reconstructions using ab initio DFT calculations. The DFT relaxations give a more accurate idea about the relative stability of the reconstructions found, and helps identify the most likely lowest-energy candidates which are shown in Fig. 4(a) and (b). As it turns out, the two models coincide with those proposed by Jeong and coworkers [14] from STM experiments and density functional calculations: this finding lends strong support to the minimization approach taken here and shows that sampling the configuration space using the HOEP potential [20] is a versatile way to find good candidate reconstructions for high-index Si surfaces. We hope that the development of algorithms for surface structure determination [16, 17] would also stimulate further research towards interatomic potentials with improved transferability, since the use of such potentials will improve the quality of the model structures found during

the global optimization: in turn, this would increase the range of materials problem since the search algorithm can be used to gain knowledge of optimal structure.

The DFT surface energies of the (337) models shown in Fig. 4(a,b) are relatively small, being about 1 meV/ Å^2 higher than the surface energy of Si(114) computed using the same computational parameters Section 2. In experiments, particular conditions can readily appear such as to favor the stabilization of Si(337) over Si(5 5 12), as shown for instance in Refs. [3, 4]. Recent works by Baski and coworkers [27] reveal a controlled way in which Si(337) facets can be formed (the deposition of gold). At Au coverages of 0.15 ML, the (5 5 12) orientation facets into Si(113) and Si(337), with the (337) surface unit cells being twice as large as the ones in Fig. 1 along the [776] direction. Since the Au coverages at which Si(337) emerges correspond to only a couple of Au atoms per each (337) unit, the models presented here can be used as building blocks for the structure of Si(337)-Au nanofacets observed in [27], as well as in other experimental situations.

Acknowledgments. CVC thanks J. Dabrowski, M. Takeguchi, and S. Jeong for correspondence on their model structures [25, 11, 14]. Ames Laboratory is operated for the U.S. Department of Energy by Iowa State University under Contract No. W-7405-Eng-82; this work was supported by the Director of Energy Research, Office of Basic Energy Sciences. We gratefully acknowledge grants of supercomputer time from EMSL at Pacific Northwest National Laboratory, from NCSA, and from NERSC.

References

- [1] Z. Gai, R. G. Zhao, W. J. Li, Y. Fujikawa, T. Sakurai, and W. S. Yang, *Phys. Rev. B* **64**, 125201 (2001).
- [2] A. A. Baski, S. C. Erwin, and L. J. Whitman, *Surf. Sci.* **392**, 69 (1997).
- [3] W. Ranke and Y. R. Xing, *Phys. Rev. B* **31**, 2246 (1985).
- [4] J. G. E. Gardeniers, W. E. J. R. M. Maas, R. Z. C. van Meerden, and L. J. Giling, *J. Cryst. Growth* **96**, 821 (1989).
- [5] X. M. Hu, E. G. Wang, and Y. R. Xing, *Appl. Surf. Sci.* **103**, 217 (1996).
- [6] A. A. Baski and L. J. Whitman, *Phys. Rev. Lett.* **74**, 956 (1995).
- [7] A. A. Baski and L. J. Whitman, *J. Vac. Sci. Technol. A* **13**, 1469 (1995).
- [8] A. A. Baski and L. J. Whitman, *J. Vac. Sci. Technol. B* **14**, 992 (1996).
- [9] A. A. Baski, S. C. Erwin, and L. J. Whitman, *Science* **269**, 1556 (1995).
- [10] S. Song, M. Yoon, and S. G. J. M. Odrrie, *Surf. Sci.* **334**, 153 (1995).

[11] M . Takeguchi, Y . W u, and K . Furuya, *Surf. Interf. Anal.* 30, 288 (2000).

[12] W . Ranke and Y R . X ing, *Surf. Rev. Lett.* 4, 15 (1997).

[13] J. Liu, M . Takeguchi, H . Yasuda, and K . Furuya, *J. Cryst. Growth*, 237, 188 (2002).

[14] S . Jeong, H . Jeong, S . Cho, and J.M . Seo, *Surf. Sci.* 557, 183 (2004).

[15] C V . Ciobanu, V B . Shenoy, C Z .W ang, and K M .H o, *Surf. Sci.* 544, L715 (2003).

[16] C V . Ciobanu and C .P redescu, *Phys. Rev. B* 70, 085321 (2004).

[17] F C .C huang, C V .C iobanu, V B .Shenoy, C Z .W ang, and K M .H o, *Surf. Sci.* 573, L375 (2004).

[18] F C .C huang, C V .C iobanu, C .P redescu, C Z .W ang, and K M .H o, *Surf. Sci.* 578, 183 (2005).

[19] T W . Poon, S .Y ip, P S .H o, and F F .A braham , *Phys. Rev. B* 45, 3521 (1992).

[20] T J .L enosky, B .S adigh, E .A lonso, V V .B ulatov, T .D iaz de la R ubia, J. K im , A F .V oter, and J D .K ress, *M odelling Simul. Mater. Sci. Eng.* 8, 825 (2000).

[21] H J W . Zandvliet, *Surf. Sci.* 577, 93 (2005).

[22] S .B aroni, A .D alC orso, S .de G ironcoli, and P .G iannozzi, < <http://www.pwscf.org> > .

[23] J P .P erdew and A .Zunger, *Phys. Rev. B* 23, 5048 (1981)

[24] S C .E rw in, A A .B aski, and L J .W hitman, *Phys. Rev. Lett.* 77, 687 (1996).

[25] J. D abrowski, H J .M ussig, G .W ol , *Phys. Rev. Lett.* 73, 1660 (1994).

[26] C V .C iobanu, D T .T ambe, V B .Shenoy, C Z .W ang, and K M .H o, *Phys. Rev. B* 68, 201302 (2003).

[27] A A .B aski and K M .Saoud, *J. Cluster Sci.* 12, 527 (2001); J W .D ickinson, J C .M oore and A A .B aski, *Surf. Sci.* 561, 193 (2004).